Materials Science

http://www.aimspress.com/

AIMS Materials Science, 2(4): 401–413.
DOI:10.3934/matersci.2015.4.401
Received 23 July 2015
Accepted 19 October 2015
Published 26 October 2015

Research article

Detection and response characteristics of clamped-free giant magnetostrictive/piezoelectric laminates under concentrated loading

Kotaro Mori[1,*], **Fumio Narita**[2] , **and Yasuhide Shindo**[2]

[1] Department of Mechanical Engineering, College of Engineering, Ibaraki University, Nakanarusawa-cho 4-12-1, Hitachi, Ibaraki 316-8511, Japan

[2] Department of Materials Processing, Graduate School of Engineering, Tohoku University, Aoba-yama 6-6-02, Sendai, Miyagi 980-8579, Japan

[*] **Correspondence:** mori-k@mx.ibaraki.ac.jp; Tel: +81-294-38-5043.

Abstract: This work deals with the detection and response characteristics of clamped-free giant magne-tostrictive/piezoelectric laminates under concentrated loading both numerically and experimentally. The laminate is fabricated using thin magnetostrictive Terfenol-D and piezoelectric PZT layers. Three dimensional finite element analysis was carried out, and the electromagneto-mechanical fields in the two and three layered magnetostrictive/piezoelectric laminates were predicted by introducing a second-order magnetoelastic constant of Terfenol-D. The tip deflection, induced voltage and induced magnetic field were also measured, and comparison was made between simulation and experiment to verify the model.

Keywords: electromagneto-solid mechanics; finite element method; material testing; electronic laminates; smart materials and structures; bending

1. Introduction

Magnetostrictive materials have been studied due to their great potential as sensor and actuator elements in a wide variety of applications that can benefit from their remote operation, high energy density and short response time [1]. Among giant magnetostrictive materials, Terbium Dysprosium Iron alloy (Terfenol-D) is the most attractive one because of its high saturation magnetostrain (1600 ppm), good coupling coefficient (as high as 60%), and high Young's modulus [2]. On the other hand, piezoelectric ceramics, especially lead zircornate titanate (PZT), are widely used in smart materials and structures due to their high output force, compact size, and high power density. Magnetoelectric (ME) composites require giant magnetostrictive and piezoelectric materials, with a strong coupling between them, and many applications of these composites such as magnetic field sensing devices [3,4], coil-less

transformers and read/write devices [5] are currently under investigation.

Recently, energy harvesting devices can be used as the power source for structural health monitoring sensors, tire pressure monitoring sensors, medical implants and other wireless sensors. The devices of energy harvesting from ambient sources, such as mechanical loads, provide a promising alternative to battery-powered systems. Gao et al. [6] discussed the effect of the length ratio between the substrate layer and the piezoelectric layer on the induced voltage of the PZT/stainless steel cantilevers due to a constant force. Hu et al. [7] designed and tested an optimal vibration-based energy harvesting system using magnetostrictive material. Dai et al. [8] investigated the performances of electric output due to vibration in three layered magnetostrictive/piezoelectric composite harvesters.

Energy harvesting magnetostrictive/piezoelectric laminates are subjected to high mechanical loads, and these loads cause high response levels that increase the generated power but induce the delamination and reduce the lifetime of the laminates. In this work, we study the detection and response characteristics of clamped-free giant magnetostrictive/piezoelectric laminates under concentrated loading in a combined numerical and experimental approach. Two and three layered laminates are fabricated by bonding Terfenol-D layers on one side and both sides of PZT layer, respectively. The tip deflection, stress, induced voltage and induced magnetic field for the laminates due to concentrated loads are calculated by the finite element analysis (FEA). The tip deflection, induced voltage and induced magnetic field are also measured, and the data produced by the experiment are then compared with analytical results.

2. Analysis

2.1. Basic equations

The basic equations for magnetostrictive and piezoelectric materials are outlined here. The equilibrium equations in the rectangular Cartesian coordinate system O-$x_1x_2x_3$ are given by

$$\sigma_{ji,j} = 0 \tag{1}$$

$$B_{i,i} = 0 \tag{2}$$

$$D_{i,i} = 0 \tag{3}$$

where σ_{ij} is the stress tensor, B_i is the magnetic induction vector, D_i is the electric displacement vector, a comma followed by an index denotes partial differentiation with respect to the space coordinate x_i, and the summation convention for repeated tensor indices is applied. The constitutive laws are given as follows:

$$\varepsilon_{ij} = s^H_{ijkl}\sigma_{kl} + d'_{kij}H_k \tag{4}$$

$$B_i = d'_{ikl}\sigma_{kl} + \mu_{ik}H_k \tag{5}$$

for the magnetostrictive material, and

$$\varepsilon_{ij} = s^E_{ijkl}\sigma_{kl} + d_{kij}E_k \tag{6}$$

$$D_i = d_{ikl}\sigma_{kl} + \epsilon^T_{ik}E_k \tag{7}$$

for the piezoelectric material. Here, ε_{ij} is the strain tensor, H_i is the magnetic field intensity vector, E_i is the electric field intensity vector, $s^H_{ijkl}, d'_{kij}, \mu_{ij}$ are the constant magnetic field elastic compliance, magnetoelastic constant and magnetic permittivity of magnetostrictive material, and $s^E_{ijkl}, d_{kij}, \epsilon^T_{ij}$ are the constant electric field elastic compliance, direct piezoelectric constant and dielectric permittivity of piezoelectric material. Valid symmetry conditions for the material constants are

$$s^H_{ijkl} = s^H_{jikl} = s^H_{ijlk} = s^H_{klij}, \quad d'_{kij} = d'_{kji}, \quad \mu_{ij} = \mu_{ji} \tag{8}$$

$$s^E_{ijkl} = s^E_{jikl} = s^E_{ijlk} = s^E_{klij}, \quad d_{kij} = d_{kji}, \quad \epsilon^T_{ij} = \epsilon^T_{ji} \tag{9}$$

The relation between the strain tensor and the displacement vector u_i is given by

$$\varepsilon_{ij} = \frac{1}{2}(u_{j,i} + u_{i,j}) \tag{10}$$

The magnetic and electric field intensities are written as

$$H_i = \varphi_{,i} \tag{11}$$

$$E_i = -\phi_{,i} \tag{12}$$

where φ and ϕ are the magnetic and electric potentials, respectively.

2.2. Model

Two layered magnetostrictive/piezoelectric laminate is shown in Figure 1(a), in which a magnetostrictive layer, Terfenol-D, of length l_m = 15 mm, width w_m = 5 mm and thickness h_m = 1 and 3 mm is perfectly bonded on the upper surface of a piezoelectric layer, PZT, of length l_p = 20 mm, width w_p = 5 mm and thickness h_p = 0.5 mm. We will use subscripts m and p to refer to Terfenol-D and PZT layers, respectively. Dimensions $h_m(h_p)$, $w_m(w_p)$, $l_m(l_p)$ are measured along the $x_1 = x$, $x_2 = y$ and $x_3 = z$ axis, respectively. The origin of the coordinate system is located at the center of the bottom left side of upper Terfenol-D layer, and the left end $z = 0$ is clamped. Three layered laminate is also considered (see Figure 1(b)). Easy axis of the magnetization of Terfenol-D layer is the z-direction, while the polarization of PZT layer is the x-direction. The constitutive relations for Terfenol-D and PZT layers are given in Appendix A.

As we know, a magnetic domain switching gives rise to the changes of the magnetoelastic constants [9], and the constants d'_{15}, d'_{31} and d'_{33} for Terfenol-D layer in the z-direction magnetic field are

$$\begin{aligned} d'_{15} &= d^m_{15} \\ d'_{31} &= d^m_{31} + m_{31}H_z \\ d'_{33} &= d^m_{33} + m_{33}H_z \end{aligned} \tag{13}$$

where $d^m_{15}, d^m_{31}, d^m_{33}$ are the piezo-magnetic constants, and m_{31} and m_{33} are the second-order magnetoelastic constants. When the length of Terfenol-D is much longer than other two sizes (width and thickness) and a magnetic field is along the length direction (easy axis), the longitudinal (33) magnetostrictive deformation mode is dominant. So it is assumed that only the constant d'_{33} varies with magnetic field [10], and the constant m_{31} equals to zero.

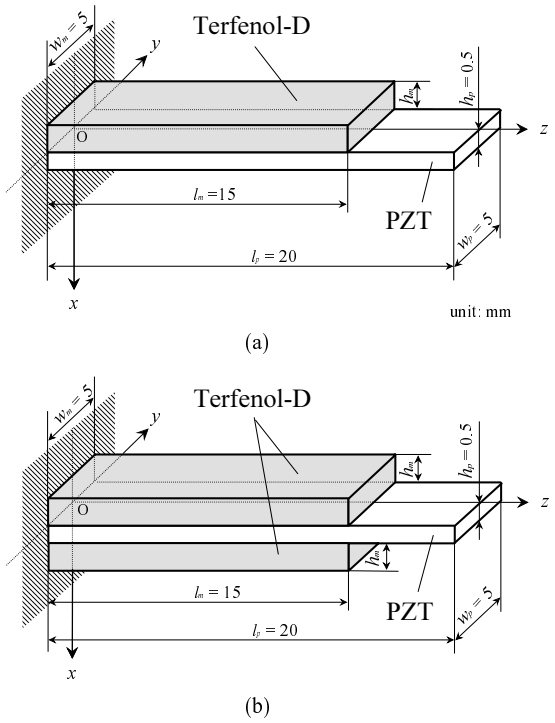

Figure 1. Illustration of (a) two-layered and (b) three-layered magnetostrictive/piezoelectric laminate configurations.

We performed finite element calculations to obtain the tip deflection, stress, induced voltage and induced magnetic field for the magnetostrictive/piezoelectric laminates. The average induced magnetic field in the z-direction at the side surface (at $z = l_m$ plane) is calculated as

$$B_{\text{in}} = \frac{1}{A}\int_A B_z(x, y, l_m)dA \tag{14}$$

where the integration is over the surface area, $A = w_m h_m$, of Terfenol-D layer. The basic equations for the magnetostrictive materials are mathematically equivalent to those for piezoelectric materials. So coupled-field solid elements in ANSYS were used in the analysis. Only a half of the laminate was modeled. In total, 15500 and 27500 elements and 18931 and 32291 nodes were used for h_m = 1 and 3 mm of two-layered model, respectively. For three-layered model, 23000 and 47000 elements and 27236 and 53812 nodes were used for h_m = 1 and 3 mm, respectively. It should be noted that before carrying out simulations, a mesh sensitivity study was performed to ensure that the mesh was fine enough. The finite element computations were provided by modifying the program with routines developed by our previous works [11,12].

3. Materials and Methods

Terfenol-D (Etrema Products, Inc., USA) of l_m = 15 mm, w_m = 5 mm, h_m = 1 and 3 mm and PZT C-91 (Fuji Ceramics, Co. Ltd., Japan) of l_p = 20 mm, w_p = 5 mm, h_p = 0.5 mm were used to make giant magnetostrictive/piezoelectric laminates by epoxy bonding (EP-34B; Kyowa Electronic Instruments Co. Ltd., Japan). Owing to cost and time constrains, the number of specimens (one or two at each types and thicknesses) was limited. It is noted that Terfenol-D is a rare earth iron and very expensive. Table 1 and Table 2 list the material properties of Terfenol-D [13,14] and C-91 [15], respectively. The second-order magnetoelastic constants m_{33} of Terfenol-D layer with h_m = 1 and 3 mm of two-layered laminate are 5.0 $\times 10^{-12}$ and 3.3 $\times 10^{-12}$ m^2/A^2 [11], and the constants m_{33} of h_m = 1 and 3 mm of three-layered laminate are 5.2 $\times 10^{-12}$ and 2.3 $\times 10^{-12}$ m^2/A^2 [12], respectively.

Consider magnetostrictive/piezoelectric laminates under concentrated loading. Figure 2 and 3, for example, shows the setup for the experiment of a two-layered laminate (Figure 1(a)). Concentrated load P_0 was applied at $x = y = 0$, $z = l_p$ by the cantilever load cell [6], as shown in Figure 2. First, the displacement for the two-layered and three-layered laminates under concentrated loading was measured with a laser displacement meter (see Figure 3(a)). Next, the induced voltage of these laminates was measured using an oscilloscope (see Figure 3(b)). The $x = h_p$ plane was grounded. Then, the induced magnetic field over the total area on $z = l_m$ plane of Terfenol-D layer was measured using a Tesla meter (see Figure 3(c)). The hall probe was touched on the edge of Terfenol-D layer, and this set-up allowed a precision of induced magnetic field measurement of ± 0.01 mT.

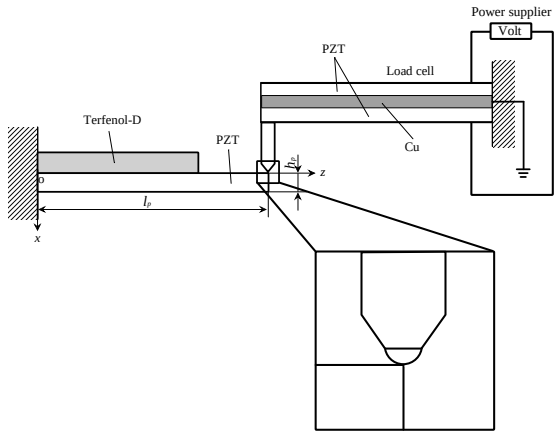

Figure 2. Diagram of the experimental setup.

Table 1. Material properties of Terfenol-D.

	Elastic compliance ($\times 10^{-12} m^2/N$)					Piezo-magnetic constant ($\times 10^{-9} m/A$)			Magnetic permittivity ($\times 10^{-6} H/m$)	
	s_{11}^H	s_{33}^H	s_{44}^H	s_{12}^H	s_{13}^H	d_{31}^m	d_{33}^m	d_{15}^m	μ_{11}	μ_{33}
Terfenol-D	17.9	17.9	26.3	−5.88	−5.88	−5.3	11	28	6.29	6.29

Table 2. Material properties of C-91.

	Elastic compliance ($\times 10^{-12}$m^2/N)					Direct piezoelectric constant ($\times 10^{-12}$m/V)			Dielectric permittivity ($\times 10^{-10}$C/Vm)	
	s_{11}^E	s_{33}^E	s_{44}^E	s_{12}^E	s_{13}^E	d_{31}	d_{33}	d_{15}	ϵ_{11}^T	ϵ_{33}^T
C-91	17.1	18.6	41.4	−6.3	−7.3	−340	645	836	395	490

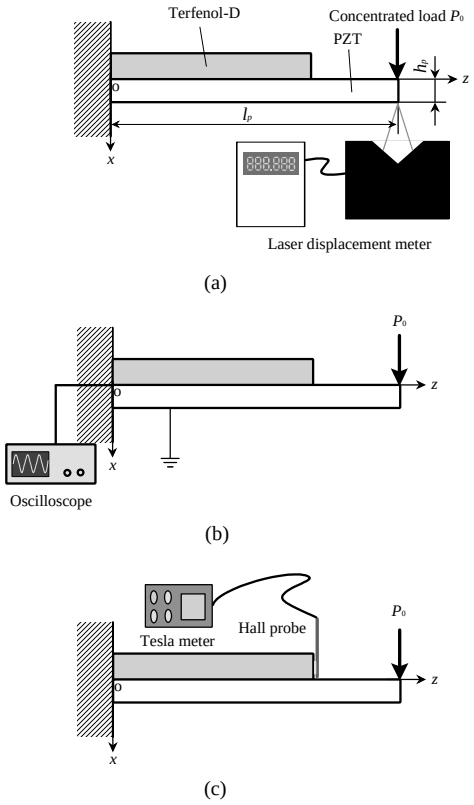

Figure 3. Experimental setup for measuring (a) the tip deflection, (b) the induced voltage and (c) the induced magnetic field.

4. Results and Discussion

We first present results for the two-layered magnetostirctive/piezoelectric laminates. Figure 4 shows the tip deflection w_{tip} versus applied concentrated load P_0 at $x = h_p$, $y = 0$, $z = l_p$ for the two-layered laminates with $h_m = 1$ and 3 mm. The lines and plots denote the results of FEA and test. The experimental scatter is small, and the representative plots from the tests are shown. The tip deflection increases as the thickness of the Terfenol-D layer decreases. The FEA results are good agreement with experimental measurements. Figure 5 shows the induced voltage V_{in} versus applied concentrated load P_0 at $x = 0$ plane for the two-layered laminates with $h_m = 1$ and 3 mm, obtained from the FEA and test. As the concentrated load increases, the induced voltage increases. The comparison between the numerical predictions and the experimental results for the two-layered laminate with $h_m = 3$ mm yields

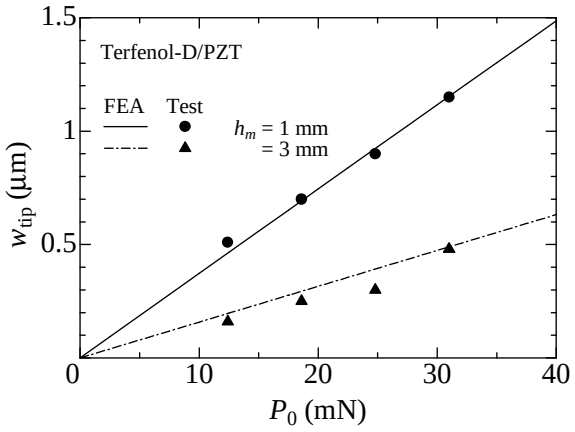

Figure 4. Tip deflection versus concentrated load at $x = h_p$, $y = 0$, $z = l_p$ for two-layerd magnetostrictive/piezoelectric laminates.

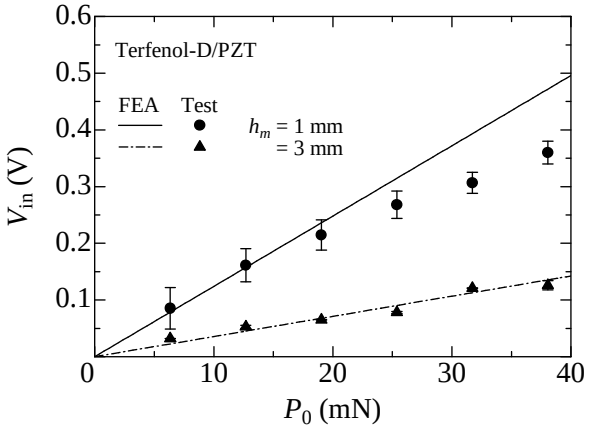

Figure 5. Induced voltage versus concentrated load at $x = 0$ plane for two-layered magnetostrictive/piezoelectric laminates.

a good agreement. For the laminate with $h_m = 1$ mm, the trend is similar between the numerical predictions and the experimental results, though the experimental data are smaller than the predicted ones because of the voltage saturation under high mechanical loads. Figure 6 shows the induced magnetic field B_{in} versus applied concentrated load P_0 for the two-layered laminates with $h_m = 1$ and 3 mm, obtained from the FEA. Also shown are the measured data for $h_m = 3$ mm. The comparison between the FEA and test is reasonable. As the concentrated load increases, the induced magnetic field increases. The induced magnetic field increases as the thickness of the Terfenol-D layers decreases. The variations of normal stress σ_{zz} along the thickness direction are calculated at the clamped end ($y = 0$ mm and $z = 0$ mm) for the two-layered laminates and the results are shown in Figure 7. All calculations are done at a fixed tip deflection of $w_{tip} = 1$ μm. The applied loads of PZT layer for $w_{tip} = 1$ μm are about $P_0 = 27.0$, 62.7 mN for $h_m = 1$ and 3 mm, and the corresponding induced voltage and

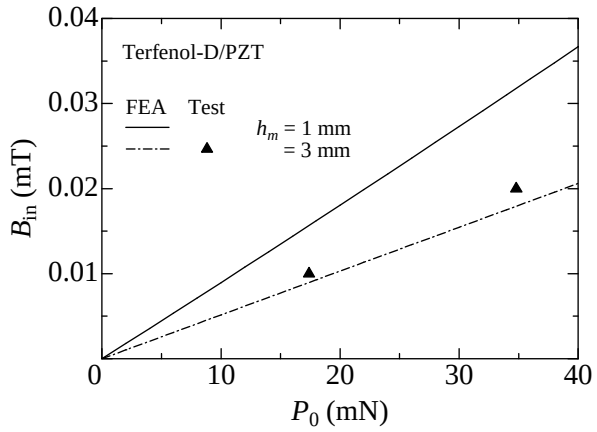

Figure 6. Induced magnetic field versus concentrated load at $z = l_m$ plane for two-layerd magnetostrictive/piezoelectric laminates.

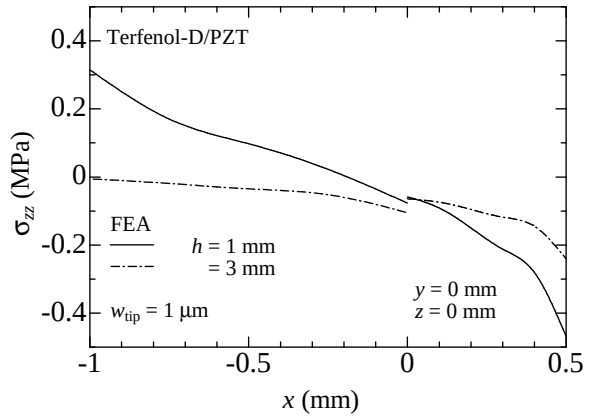

Figure 7. Normal stress distribution along the thickness direction at $y = 0$ and $z = 0$ mm for two-layered magnetostrictive/piezoelectric laminates at a tip deflection of 1 μm.

induced magnetic field are about V_{in} = 0.338, 0.229 V and B_{in} = 0.024, 0.032 mT, respectively. Small stress gaps at the interface between Terfenol-D and PZT layers are observed. Figure 8 also shows the variations of normal stress σ_{zz} along the thickness direction near the free edge of Terfenol-D layer (y = 0 mm and z = 14.5 mm) for the two-layered laminates at the same condition. The normal stress in Terfenol-D layer is almost zero and the normal stress in PZT layer changes from tensile to compressive. There are some stress gaps at the interface between Terfenol-D and PZT layers. Figure 9 shows the variations of shear stress σ_{xz} along the length direction at the interface between Terfenol-D and PZT layers (x = 0 mm and y = 0 mm) for the two-layered laminates at the same condition. The maximum shear stress is observed near the free edge of Terfenol-D layer. Low shear stress is noted for small Terfenol-D layer thickness.

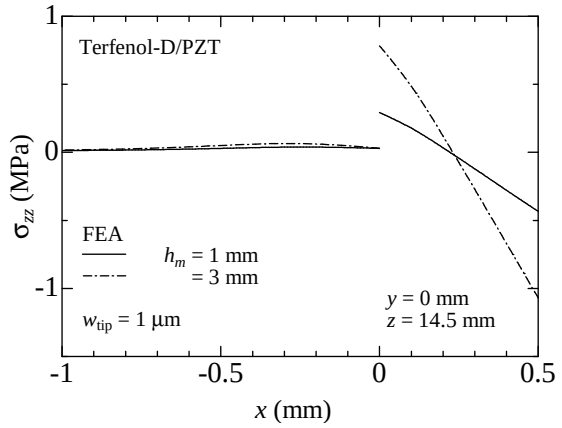

Figure 8. Normal stress distribution along the thickness direction at y = 0 and z = 14.5 mm for two-layered magnetostrictive/piezoelectric laminates at a tip deflection of 1 μm.

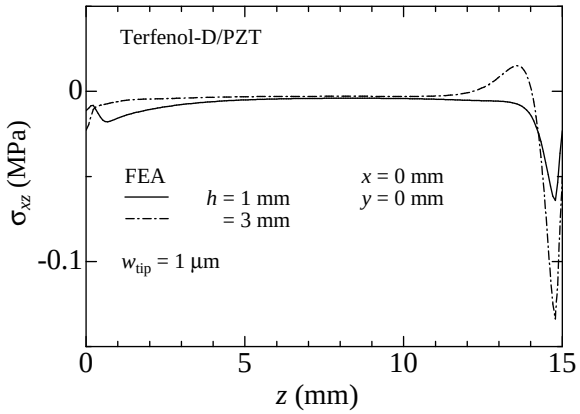

Figure 9. Shear stress distribution along the length direction at x = 0 and y = 0 mm for two-layered magnetostrictive/piezoelectric laminates at a tip deflection of 1 μm.

Next, the results of the three-layered magnetostrictive/piezoelectric laminates are presented. Figure 10 shows the tip deflection w_{tip} versus applied concentrated load P_0 at $x = h_p$, $y = 0$, $z = l_p$ for the three-layered laminates with h_m = 1 and 3 mm. The lines and plots denote the results of FEA and test. The experimental scatter is small, and the representative plots from the tests are shown. The tip deflection for h_m = 1 mm is larger than that for h_m = 3 mm, and both the numerical predictions and the experimental results show a same tendency. Figure 11 shows the induced voltage V_{in} versus applied concentrated load P_0 for the three-layered laminate with h_m = 3 mm. Also shown is the induced magnetic field B_{in}. Only one datum for B_{in} is plotted due to the accuracy limit of the Tesla meter. As the concentrated load increases, both the induced voltage and the induced magnetic field increase. The induce voltage of the two-layered laminate was much larger than that of the three-layered laminate. In addition, the induced voltage increases with decrease in the thickness of magnetostrictive layers. It stems from the facts that two-layered laminate and thin magnetostrictive layers are more easily deformed than three-layered laminate and thick magnetostrictive layers. However, if the thickness of

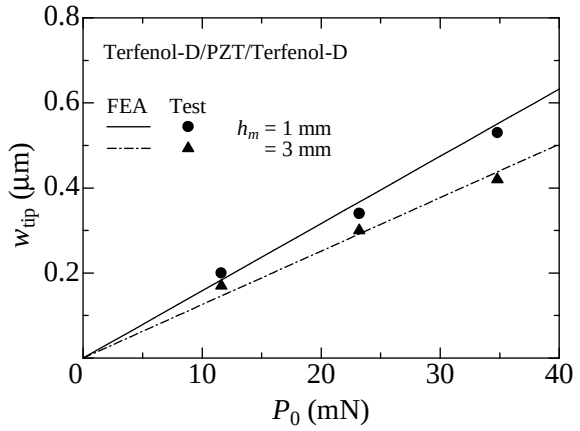

Figure 10. Tip deflection versus concentrated load at $x = h_p$, $y = 0$, $z = l_p$ for three-layerd magnetostrictive/piezoelectric laminates.

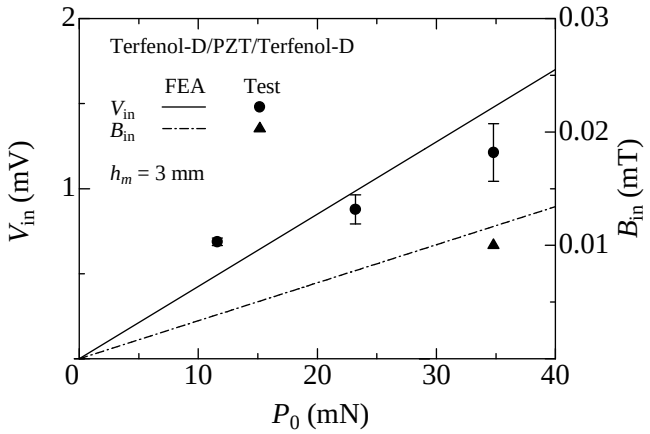

Figure 11. Induced voltage and induced magnetic field versus concentrated load for three-layerd magnetostrictive/piezoelectric laminate with $h_m = 3$ mm.

the Terfenol-D layer is reduced to several micrometers or more less, induced voltage decreases because the volume effect on the magnetization is more dominant than the magnetic field generation by deformation. The variations of normal stress σ_{zz} along the thickness direction are calculated near the free edge of Terfenol-D layer (y = 0 mm and z = 14.5 mm) for the three-layered laminates and the results are shown in Figure 12. All calculations are done at a fixed tip deflection of $w_{\text{tip}} = 1$ μm. The applied loads of PZT layer for $w_{\text{tip}} = 1$ μm are about P_0 = 62.7, 78.3 mN for h_m = 1 and 3 mm, and the corresponding induced voltage and induced magnetic field are about V_{in} = 2.64, 3.30 mV and B_{in} = 0.051, 0.026 mT, respectively. There are some stress gaps at the interface between Terfenol-D and PZT layers. At smaller Terfenol-D layer thickness, lower stress gap is found for the same tip deflection. The normal stress in Terfenol-D layer is almost zero and the normal stress in PZT layer changes from tensile to compressive.

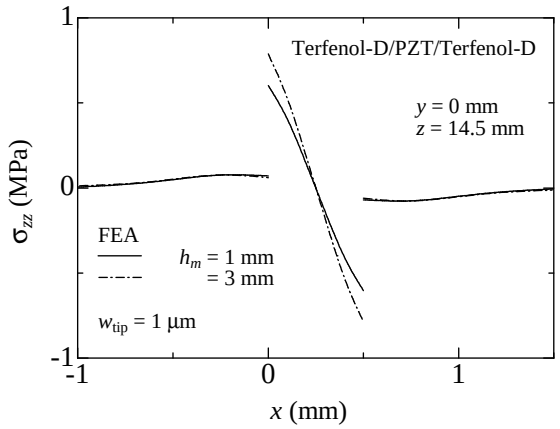

Figure 12. Normal stress distribution along the thickness direction at y = 0 and z = 14.5 mm for three-layered magnetostrictive/piezoelectric laminates at a tip deflection of 1 μm.

These results are helpful in considering the energy harvesting from impact. And, it is important that the internal stress is evaluated for fracture and delamination of the laminates also. Our present study offers a method for aiding the design of new energy harvesting devices, and provides a rational basis for refining the real device designing in order to reduce fracture and increase efficiency of electric power generation. Work in this area is currently being pursued.

5. Conclusion

A numerical and experimental investigation of the magnetostrictive/piezoelectric laminates under concentrated loading was conducted. The tip deflection, induced voltage and induced magnetic field are predicted using finite element simulations, and comparison with the measured data shows that current predictions are reasonable. It was found that smaller magnetostrictive layer thickness gives larger tip deflection, induced voltage and induced magnetic field. Also, the induce voltage of the two-layered laminate was much larger than that of the three-layered laminate. In addition, the stress gap at the interface is small when the magnetostrictive layer thickness is small. This study may be useful in designing advanced magnetostrictive/piezoelectric laminates with energy harvesting capabilities.

Acknowledgments

This work was supported by Grant-in-Aid for JSPS Fellows (23-3402).

Conflict of Interest

All authors declare no conflicts of interest in this paper.

Appendix A

For Terfenol-D, the constitutive relations can be written in the following form:

$$\begin{Bmatrix} \varepsilon_{xx} \\ \varepsilon_{yy} \\ \varepsilon_{zz} \\ \varepsilon_{yz} \\ \varepsilon_{zx} \\ \varepsilon_{xy} \end{Bmatrix} = \begin{bmatrix} s_{11}^H & s_{12}^H & s_{13}^H & 0 & 0 & 0 \\ s_{12}^H & s_{11}^H & s_{13}^H & 0 & 0 & 0 \\ s_{13}^H & s_{13}^H & s_{33}^H & 0 & 0 & 0 \\ 0 & 0 & 0 & s_{44}^H/2 & 0 & 0 \\ 0 & 0 & 0 & 0 & s_{44}^H/2 & 0 \\ 0 & 0 & 0 & 0 & 0 & s_{66}^H/2 \end{bmatrix} \begin{Bmatrix} \sigma_{xx} \\ \sigma_{yy} \\ \sigma_{zz} \\ \sigma_{yz} \\ \sigma_{zx} \\ \sigma_{xy} \end{Bmatrix} + \begin{bmatrix} 0 & 0 & d'_{31} \\ 0 & 0 & d'_{31} \\ 0 & 0 & d'_{33} \\ 0 & d'_{15}/2 & 0 \\ d'_{15}/2 & 0 & 0 \\ 0 & 0 & 0 \end{bmatrix} \begin{Bmatrix} H_x \\ H_y \\ H_z \end{Bmatrix} \tag{A.1}$$

$$\begin{Bmatrix} B_x \\ B_y \\ B_z \end{Bmatrix} = \begin{bmatrix} 0 & 0 & 0 & 0 & d'_{15} & 0 \\ 0 & 0 & 0 & d'_{15} & 0 & 0 \\ d'_{31} & d'_{31} & d'_{33} & 0 & 0 & 0 \end{bmatrix} \begin{Bmatrix} \sigma_{xx} \\ \sigma_{yy} \\ \sigma_{zz} \\ \sigma_{yz} \\ \sigma_{zx} \\ \sigma_{xy} \end{Bmatrix} + \begin{bmatrix} \mu_{11} & 0 & 0 \\ 0 & \mu_{11} & 0 \\ 0 & 0 & \mu_{33} \end{bmatrix} \begin{Bmatrix} H_x \\ H_y \\ H_z \end{Bmatrix} \tag{A.2}$$

where

$$\left.\begin{array}{l} s_{11}^H = s_{1111}^H = s_{2222}^H,\ s_{12}^H = s_{1122}^H,\ s_{13}^H = s_{1133}^H = s_{2233}^H,\ s_{33}^H = s_{3333}^H \\ s_{44}^H = 4s_{2323}^H = 4s_{3131}^H,\ s_{66}^H = 4s_{1212}^H = 2(s_{11}^H - s_{12}^H) \end{array}\right\} \tag{A.3}$$

$$d'_{15} = 2d'_{131} = 2d'_{223},\ \ d'_{31} = d'_{311} = d'_{322},\ \ d'_{33} = d'_{333} \tag{A.4}$$

The constitutive relations for PZT (hexagonal crystal of class 6mm) are

$$\begin{Bmatrix} \varepsilon_{xx} \\ \varepsilon_{yy} \\ \varepsilon_{zz} \\ \varepsilon_{yz} \\ \varepsilon_{zx} \\ \varepsilon_{xy} \end{Bmatrix} = \begin{bmatrix} s_{33}^E & s_{13}^E & s_{13}^E & 0 & 0 & 0 \\ s_{13}^E & s_{11}^E & s_{12}^E & 0 & 0 & 0 \\ s_{13}^E & s_{12}^E & s_{11}^E & 0 & 0 & 0 \\ 0 & 0 & 0 & s_{66}^E/2 & 0 & 0 \\ 0 & 0 & 0 & 0 & s_{44}^E/2 & 0 \\ 0 & 0 & 0 & 0 & 0 & s_{44}^E/2 \end{bmatrix} \begin{Bmatrix} \sigma_{xx} \\ \sigma_{yy} \\ \sigma_{zz} \\ \sigma_{yz} \\ \sigma_{zx} \\ \sigma_{xy} \end{Bmatrix} + \begin{bmatrix} d_{33} & 0 & 0 \\ d_{31} & 0 & 0 \\ d_{31} & 0 & 0 \\ 0 & 0 & 0 \\ 0 & 0 & d_{15}/2 \\ 0 & d_{15}/2 & 0 \end{bmatrix} \begin{Bmatrix} E_x \\ E_y \\ E_z \end{Bmatrix} \tag{A.5}$$

$$\begin{Bmatrix} D_x \\ D_y \\ D_z \end{Bmatrix} = \begin{bmatrix} d_{33} & d_{31} & d_{31} & 0 & 0 & 0 \\ 0 & 0 & 0 & 0 & 0 & d_{15} \\ 0 & 0 & 0 & 0 & d_{15} & 0 \end{bmatrix} \begin{Bmatrix} \sigma_{xx} \\ \sigma_{yy} \\ \sigma_{zz} \\ \sigma_{yz} \\ \sigma_{zx} \\ \sigma_{xy} \end{Bmatrix} + \begin{bmatrix} \epsilon_{33}^T & 0 & 0 \\ 0 & \epsilon_{11}^T & 0 \\ 0 & 0 & \epsilon_{11}^T \end{bmatrix} \begin{Bmatrix} E_x \\ E_y \\ E_z \end{Bmatrix} \tag{A.6}$$

where

$$\left.\begin{array}{l} s_{11}^E = s_{2222}^E = s_{3333}^E,\ s_{12}^E = s_{2233}^E,\ s_{13}^E = s_{1122}^E = s_{1133}^E,\ s_{33}^E = s_{1111}^E \\ s_{44}^E = 4s_{1212}^E = 4s_{1313}^E,\ s_{66}^E = 4s_{2323}^E = 2(s_{11}^E - s_{12}^E) \end{array}\right\} \tag{A.7}$$

$$d_{15} = 2d_{313} = 2d_{212},\ \ d_{31} = d_{122} = d_{133},\ \ d_{33} = d_{111} \tag{A.8}$$

References

1. Valadkhan S, Morris K, Khajepour A (2009) Review and comparison of hysteresis models for magnetostrictive materials. *J Intell Mater Syst Struct* 20: 131–142.
2. Bayrashev A, Robbins W, Ziaie B (2004) Low frequency wireless powering of microsystems using piezoelectric-magnetostrictive laminate composites. *Sens Actuator A-Phys* 114: 244–249.
3. Dong S, Bai J, Zhai J, et al. (2005) Circumferential-mode, quasi-ring-type, magnetoelectric laminate composite-a highly sensitive electric current and/or vortex magnetic field sensor. *Appl Phys Lett* 86: 182506.
4. Wang Y, Atulasimha J, Prasoon R (2010) Nonlinear magnetoelectric behavior of Terfenol-D/PZT-5A laminate composites. *Smart Mater Struct* 19: 125005.
5. Nan C, Bichurin M, Dong S, et al. (2008) Multiferroic magnetoelectric composites: Historical perspective, status, and future directions. *J Appl Phys* 103: 031101.
6. Gao X, Shih W, Shih W (2009) Induced voltage of piezoelectric unimorph cantilevers of different nonpiezoelectric/piezoelectric length ratios. *Smart Mater Struct* 18: 125018.
7. Hu J, Xu F, Huang A, et al. (2011) Optimal design of a vibration-based energy harvester using magnetostrictive material (MsM). *Smart Mater Struct* 20: 015021.
8. Dai X, Wen Y, Li P, et al. (2009) Modeling, characterization and fabrication of vibration energy harvester using Terfenol-D/PZT/Terfenol-D composite transducer. *Sens Actuators A* 156: 350–358.
9. Wan Y, Fang D, Hwang K (2003) Non-linear constitutive relations for magnetostrictive materials *Int J Non-Linear Mech* 38: 1053–1065.
10. Jia Z, Liu W, Zhang Y, et al. (2006) A nonlinear magnetomechanical coupling model of giant magnetostrictive thin films at low magnetic fields. *Sens Actuators A* 128: 158–164.
11. Mori K, Shindo Y, Narita F (2011) Electromagneto-mechanical behavior of giant magnetostrictive/piezoelectric laminates under electric fields for self-sensing cantilever actuator. *J Solid Mech Mater Eng* 5: 360–369.
12. Mori K, Narita F, Shindo Y (2011) Effect of electric field on the response of clamped-free magnetostrictive/piezoelectric/magnetostrictive laminates. *Comput Mat Contin* 23: 187–199.
13. Engdahl G (2000) Handbook of Giant Magnetostrictive Materials. San Diego : Academic Press
14. Nan C, Li M, Huang J (2001) Calculations of giant magnetoelectric effects in ferroic composites of rare-earth-iron alloys and ferroelectric polymers. *Phys Rev B* 63: 144415.
15. Narita F, Shindo Y, Hayashi K (2005) Bending and polarization switching of piezoelectric laminated actuators under electromechanical loading. *Comput Struct* 83: 1164–1170.

AIMS Press